



HAL
open science

Tangents to fractal curves and surfaces

Dmitry Sokolov, Christian Gentil, Hicham Bensoudane

► **To cite this version:**

Dmitry Sokolov, Christian Gentil, Hicham Bensoudane. Tangents to fractal curves and surfaces. 7th International Conference on Curves and Surfaces, Jun 2010, Avignon, France. pp.663-680. hal-00798910

HAL Id: hal-00798910

<https://u-bourgogne.hal.science/hal-00798910>

Submitted on 11 Mar 2013

HAL is a multi-disciplinary open access archive for the deposit and dissemination of scientific research documents, whether they are published or not. The documents may come from teaching and research institutions in France or abroad, or from public or private research centers.

L'archive ouverte pluridisciplinaire **HAL**, est destinée au dépôt et à la diffusion de documents scientifiques de niveau recherche, publiés ou non, émanant des établissements d'enseignement et de recherche français ou étrangers, des laboratoires publics ou privés.

Tangents to fractal curves and surfaces^{*}

Dmitry Sokolov, Christian Gentil, and Hicham Bensoudane

`dmitry.sokolov@loria.fr`

LORIA - Alice, Campus Scientifique, BP 239
54506 Vandoeuvre-les-Nancy Cedex, France

`christian.gentil@u-bourgogne.fr`

Laboratoire LE2I — UMR CNRS 5158
Faculté des Sciences Mirande, Aile de l'Ingénieur, 21078 DIJON Cedex

`Hicham.Bensoudane@u-bourgogne.fr`

Laboratoire LE2I — UMR CNRS 5158
Faculté des Sciences Mirande, Aile de l'Ingénieur, 21078 DIJON Cedex

Abstract. The aim of our work is to specify and develop a geometric modeler, based on the formalism of iterated function systems with the following objectives: access to a new universe of original, various, aesthetic shapes, modeling of conventional shapes (smooth surfaces, solids) and unconventional shapes (rough surfaces, porous solids) by defining and controlling the relief (surface state) and lacunarity (size and distribution of holes). In this context we intend to develop differential calculus tools for fractal curves and surfaces defined by IFS. Using local fractional derivatives, we show that, even if most fractal curves are nowhere differentiable, they admit a left and right half-tangents, what gives us an additional parameter to characterize shapes.

Keywords: fractal curve, fractal surface, local fractional derivative, iterated function systems

1 Introduction

Our long-term goal is to develop a geometric modeler based on iterative process and fractal geometry to allow designers to access a new universe of shapes. Special properties of fractal structures have led us to new concepts inexistent on classical geometric objects. Fractal curves and surfaces, for example, can have very different aspects and very different kinds of roughness. This vast variety of shapes is not accessible with polynomial curves and surfaces exactly because of their differentiability.

^{*} ACKNOWLEDGMENT: This work has been supported by French National Research Agency (ANR) through COSINUS program (project MODITERE n ANR-09-COSI-014).

To control these aspects we are led to use the concept of “geometric texture” [2]. This “geometric texture” is very tightly coupled with differentiability of curves and surfaces. We study and attempt to characterize differential behavior from a geometric point of view by means of local fractional derivative [3].

Of course, other works were performed to study differential properties of fractal curves and surfaces. Kolwankar and Gangal [12, 11] applied the fractional calculus to study real-valued functions with few examples of fractal curves. Using their results the authors are able to describe roughness of a curve with the Hölder exponent.

Cochran has proposed a method of calculating normals to a fractal surface [6]. Sealey [16] identifies C^1 fractal curves. However, these works are applicable in the cases where derivatives exist and do not permit to characterize rough shapes.

In this paper we present a general approach to study differential properties of fractal curves and surfaces. We are using BC-IFS (Boundary Controlled Iterated Function System) [19] to construct fractal structures. Then we are using this representation to study necessary and sufficient conditions of differentiability.

In order to simplify the presentation we show in detail how it can be done for the family of local corner cutting curves. Differential behaviour of these curves was studied before by De Boor [5] and Gregory [8], the cited authors have found necessary conditions of differentiability. However, BC-IFS approach allows to describe a larger family of curves, and therefore while we find the same necessary conditions for the set of curves given by De Boor, we also study other regions of the convergence domain. A cartography of domains is presented in late sections of the paper. Finally, we show that necessary conditions are also sufficient ones.

The rest of the paper is organized as follows:

- Section 2 provides necessary background needed to introduce BC-IFS in section 3.
- Section 4 studies necessary conditions of differentiability and presents cartography of the convergence domain
- Section 5 shows that necessary conditions are also sufficient ones
- Section 6 introduces a new descriptor of roughness of a fractal shape.

2 Background

2.1 IFS

Given a complete metric space (E, d) , where d is the associated metric, an *IFS* (Iterated Function System) is a finite set of contractive operators $\mathbb{T} = \{T_i\}_{i=0}^{N-1}$ acting on points of E . Each $T_i : E \rightarrow E$ induces $T_i : \mathcal{H}(E) \rightarrow \mathcal{H}(E)$, i.e. operators acting in the space $\mathcal{H}(E)$ of non-empty compact subsets of E .

Thus it is possible to define so-called Hutchinson operator $\mathbb{T} : \mathcal{H}(E) \rightarrow \mathcal{H}(E)$ as a union of operators T_i . The Hutchinson operator maps a non-empty compact $K \subset E$ onto $\bigcup_{i=0}^{N-1} T_i(K)$. The operators T_i are contractive in the space (E, d) , therefore the induced operators are contracting in the space $(\mathcal{H}(E), d_{\mathcal{H}(E)})$,

where $d_{\mathcal{H}(E)}$ is the Hausdorff metric [1]. Of course, the Hutchinson operator is also contractive in $(\mathcal{H}(E), d_{\mathcal{H}(E)})$.

The contraction theorem [9] states that there is a unique compact A such as $\mathbb{T}(A) = A$, namely the fixed point, noted $\mathcal{A}(\mathbb{T})$. Moreover, the fixed point A may be found as a limit $A = \lim_{n \rightarrow \infty} \mathbb{T}^n(K)$, where the limit does not depend on the choice of the “seed” compact K . The top line of figure 2 provides an illustration. The underlying IFS is composed of four transformations:

$$\begin{aligned} T_0 \begin{pmatrix} x \\ y \end{pmatrix} &= \begin{bmatrix} 0.85 & 0.04 \\ -0.04 & 0.85 \end{bmatrix} \begin{bmatrix} x \\ y \end{bmatrix} + \begin{bmatrix} 0.00 \\ 1.60 \end{bmatrix} & T_1 \begin{pmatrix} x \\ y \end{pmatrix} &= \begin{bmatrix} -0.15 & 0.28 \\ 0.26 & 0.24 \end{bmatrix} \begin{bmatrix} x \\ y \end{bmatrix} + \begin{bmatrix} 0.00 \\ 0.44 \end{bmatrix} \\ T_2 \begin{pmatrix} x \\ y \end{pmatrix} &= \begin{bmatrix} 0.20 & -0.26 \\ 0.23 & 0.22 \end{bmatrix} \begin{bmatrix} x \\ y \end{bmatrix} + \begin{bmatrix} 0.00 \\ 1.60 \end{bmatrix} & T_3 \begin{pmatrix} x \\ y \end{pmatrix} &= \begin{bmatrix} 0.00 & 0.00 \\ 0.00 & 0.16 \end{bmatrix} \begin{bmatrix} x \\ y \end{bmatrix} \end{aligned}$$

We have chosen a square as the seed K . Remember that the final shape is independent of the choice. Thus, at the first iteration we apply each $\{T_i\}_{i=0}^{n-1}$ to the square to get four deformed quadrilaterals in place of two branches, the stem and the top of the fern. Then we take a union of the quadrilaterals and restart the process. In few iterations only, quadrilaterals vanish being almost imperceptible, but their union being plenty engender the shape of the fern.

2.2 CIFS

In regular IFS we start from a seed, then apply a set of rules (transformations), and repeat as required. In CIFS (Controlled, or graph-directed IFS) not all rules need to be applied at each step, a directed graph controls (directs) rules [13, 15]. We associate work spaces to the nodes of the graph and the arcs represent the transformations to be applied at the current state. In such a way it is possible to blend attractors of different nature.

The left image of figure 1 represents the control graph (it can be seen as an automaton) for the regular IFS generating the Barnsley fern, the iteration process is shown in the top line of figure 2. But what happens if we modify the automaton? Let us add three more transformations to the IFS (the corresponding automaton is shown on the right of figure 1):

$$\begin{aligned} T_5 \begin{pmatrix} x \\ y \end{pmatrix} &= \begin{bmatrix} 1/2 & 0 \\ 0 & 1/2 \end{bmatrix} \begin{bmatrix} x \\ y \end{bmatrix} & T_6 \begin{pmatrix} x \\ y \end{pmatrix} &= \begin{bmatrix} 1/2 & 0 \\ 0 & 1/2 \end{bmatrix} \begin{bmatrix} x \\ y \end{bmatrix} + \begin{bmatrix} 1/2 \\ 0 \end{bmatrix} \\ T_7 \begin{pmatrix} x \\ y \end{pmatrix} &= \begin{bmatrix} 1/2 & 0 \\ 0 & 1/2 \end{bmatrix} \begin{bmatrix} x \\ y \end{bmatrix} + \begin{bmatrix} 0 \\ 1/2 \end{bmatrix} \end{aligned}$$

These three transformations on itself generate the Sierpiński’s triangle. Note also that the destination of the transformation T_2 is changed. Thus, once the transformation T_2 was applied, the subdivision is made according to the rules of the Sierpiński’s triangle. While the Barnsley’s fern consists of infinite number of shrunk copies of itself, the attractor shown in the right bottom image of figure 2 is a fern that consists of infinite number of shrunk Sierpiński’s triangles¹.

¹ In fact, the arrows of the automaton depict the data flow, or the order of application of transformations. However actual transformations act in the other direction. That

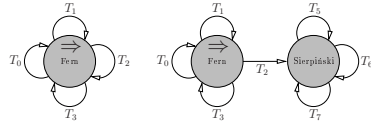


Fig. 1. Two automaton generating rules (order) of application of transformations.

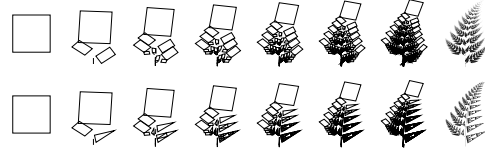


Fig. 2. Top line: the Barnsley fern; bottom line : C-IFS allows to mix up attractors of different nature.

2.3 Projected IFS

The notion of projected IFS was introduced by Zaïr and Tosan [20]. If one separates the iteration space from the modelling space, it is possible to create free-form fractal shapes. The work was inspired by spline curves, which are created by a projection of basis functions defined in a barycentric space. In the same way, it is possible to construct an IFS attractor in a barycentric space (whose dimension is equal to the number of control points) and to project it into the modelling space. In other words, if we have an attractor $A \subset BI^n = \{\lambda \in \mathbb{R}^n \mid \sum_{i=0}^{n-1} \lambda_i = 1\}$, where n is the number of control points, the projection can be made just by a matrix multiplication $PA = \{\sum_{i=0}^{n-1} P_i \lambda_i \mid \lambda_i \in A\}$. Here the matrix $P = [P_0 \ P_1 \ \dots \ P_{n-1}]$ is composed of control points. This construction imposes that transformations in IFS must act in a barycentric space. For linear operators expressed in matrix form it means that all columns sum up to 1.

3 Boundary Controlled IFS

Boundary Controlled IFS (BC-IFS) is a graph-controlled IFS with a B-rep structure introduced by Tosan et al [19]. This is a convenient method to express face-edge-vertex hierarchies implicitly existing in many fractal attractors [7]. The notions of B-rep here are a bit more general than in the classical case. Here a topological cell may be bordered by a fractal object and not only with an edge (vertex). For example, a “face” may be the Sierpiński’s triangle, an “edge” the Cantor set. The advantage of this method is its power to express incidence and adjacency constraints for subdivision processes for a given topology, what results into constraints in the subdivision matrices.

To define free-form shapes with BC-IFS it is necessary to distinguish different work spaces:

- the modeling space is where the final shape lives, this is also the space where we place control points;

is so, the right lowest branch of the new fern can be found as the following limit: $T_2(\mathcal{A}(\mathbb{T}_{5,6,7}))$, where $\mathbb{T}_{5,6,7}(K) = T_5(K) \cup T_6(K) \cup T_7(K)$. This implies that we have to choose two seeding compacts for two different spaces, in the images we have chosen a square and a triangle.

- barycentric spaces where we construct attractors corresponding to different topological entities, and this is where IFS transformations act.

Let us illustrate the approach by constructing a local corner cutting 2D or 3D curve. This type of curves demands at least 3 control points, and endpoints of a curve depend on two of them. For a curve the B-rep structure is simple: we will have edges bounded by vertices, therefore, in general case we will have four different spaces:

- \mathbb{R}^2 or \mathbb{R}^3 where the final curve is to be drawn, the control points are to be placed here
- a barycentric space of dimension 3 (we construct the simplest case with three control points), this space is where the attractor of the B-rep “edge” lives
- a barycentric space of “left” endpoint of the edge, the dimension is 2 since it depends on two control points
- similar a two-dimensional barycentric space for the “right” endpoint.

The edge and vertices are attractors in barycentric space to be projected to the modeling space, thus we need three IFS to build the attractors. Let us say that the edge is obtained with an IFS $\{T_0, T_1\}$, where T_0 and T_1 are 3×3 subdivision matrices for the edge. The vertices are obtained with IFS $\{T_{v_l}\}$ and $\{T_{v_r}\}$, and the matrices are 2×2 . Figure 4 shows the BC-IFS automaton. First of all we see four nodes corresponding to four spaces. The matrix P is the projection matrix composed of control points. The only thing we have not yet defined are transformations b_0 and b_1 .

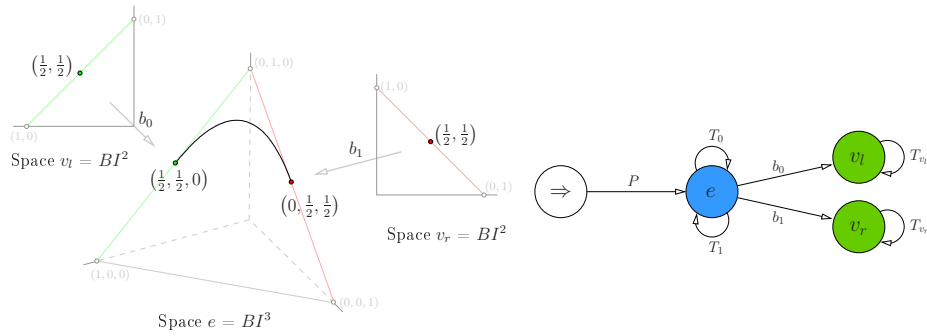


Fig. 3. At the left and at the right : barycentric spaces $v_l = v_r = BI^2$ corresponding to the vertices (left and right respectively); in the middle: edge barycentric space $e = BI^3$. The operators b_0 and b_1 embed the spaces v_l and v_r into subspaces of e .

Fig. 4. General edge-vertex B-rep BC-IFS automaton.

In fact, up to this moment we have not imposed any constraints on the IFS matrices. If we fill them with random coefficients, nothing guarantees any connectivity. However, in B-rep, vertices are boundaries of the edge, so there must be some relationship between the matrices. To ensure this we need embedding operators, namely b_0 and b_1 .

Figure 3 illustrates the approach. It shows the basis functions of a uniform B-spline quadratic curve drawn in the three-dimensional barycentric space $e = BI^3$. Basis functions for endpoints (in fact, these are just points) of the curve are drawn in corresponding two-dimensional spaces $v_l = BI^2$ and $v_r = BI^2$. Then b_0 and b_1 embed endpoint spaces into the edge space to impose that the edge has the vertices for its endpoints. Let us find shapes of b_0 and b_1 . The endpoints have coordinates $\begin{pmatrix} 1/2 \\ 1/2 \end{pmatrix}$ in the spaces v_l and v_r . At the same time in the space e they are $\begin{pmatrix} 1/2 \\ 1/2 \\ 0 \end{pmatrix}$ and $\begin{pmatrix} 0 \\ 1/2 \\ 1/2 \end{pmatrix}$. Therefore, the mappings $b_0 = \begin{pmatrix} 1 & 0 \\ 0 & 1 \\ 0 & 0 \end{pmatrix}$ and $b_1 = \begin{pmatrix} 0 & 0 \\ 1 & 0 \\ 0 & 1 \end{pmatrix}$ are indeed simple embeddings. In other words, b_0 and b_1 say on which control points depend corresponding endpoints.

3.1 Topology constraints

Incidence and adjacency constraints may be easily obtained by expanding the control graph. Figure 5 is an unfolded version of figure 4. After the first iteration on the control graph we pass from the modeling space to the edge space e , where an edge is bounded by two vertices v_l and v_r . This situation is shown in the top line of the figure. After one more iteration (bottom line) we have two smaller edges along with their own two endpoints.

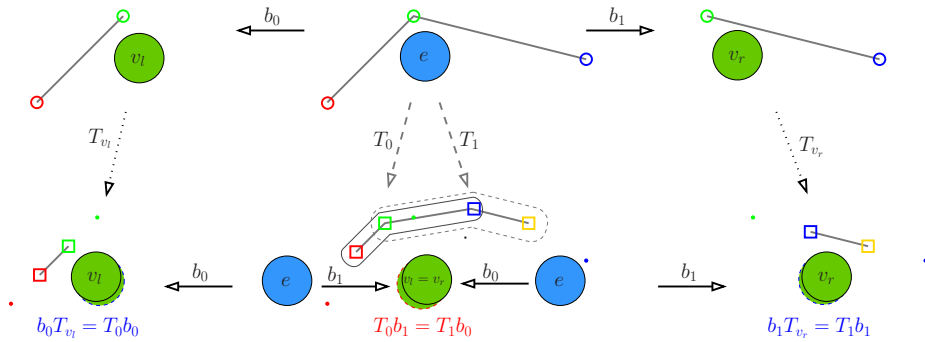


Fig. 5. Unfolded version of the control graph. This subdivision must be constrained in order to get the desired topology (here a curve). Incidence constraints are shown in red, while adjacency constraints are in blue.

Adjacency constraints Let us say that we want to get a just-touching curve. When an edge is split into two edges, the “left” subdivided edge must be connected to the “right” one in order to guarantee the topology of a curve. Therefore, we impose the “right” endpoint of the “left” edge to coincide with the “left” endpoint of the “right” edge and this implies that the “left” and “right” endpoints are of the same nature and actually live in the same space having common generating IFS. Otherwise, the connectivity will be broken at following stages of the subdivision process. So we have $T_{v_l} = T_{v_r} = T_v$.

When we say the “right” endpoint of the “left” edge this means that we can follow the path $e \xrightarrow{T_0} e \xrightarrow{b_1} v$ in the control graph. The same holds for the “left” endpoint of the “right” edge : $e \xrightarrow{T_1} e \xrightarrow{b_0} v$. As mentioned above, the vertices coincide, thus we can write $T_0 b_1 = T_1 b_0$.

Let us fill T_0 and T_1 with some arbitrary coefficients:

$$T_0 = \begin{pmatrix} a_0 & b_0 & c_0 \\ d_0 & e_0 & f_0 \\ g_0 & h_0 & i_0 \end{pmatrix} \quad T_1 = \begin{pmatrix} a_1 & b_1 & c_1 \\ d_1 & e_1 & f_1 \\ g_1 & h_1 & i_1 \end{pmatrix}$$

Then we rewrite the constraint: $T_0 b_1 = T_1 b_0$

$$\begin{pmatrix} a_0 & b_0 & c_0 \\ d_0 & e_0 & f_0 \\ g_0 & h_0 & i_0 \end{pmatrix} \begin{pmatrix} 0 & 0 \\ 1 & 0 \\ 0 & 1 \end{pmatrix} = \begin{pmatrix} a_1 & b_1 & c_1 \\ d_1 & e_1 & f_1 \\ g_1 & h_1 & i_1 \end{pmatrix} \begin{pmatrix} 1 & 0 \\ 0 & 1 \\ 0 & 0 \end{pmatrix}$$

And it implies that last two columns of T_0 are equal to two first columns of T_1 :

$$\begin{pmatrix} b_0 & c_0 \\ e_0 & f_0 \\ h_0 & i_0 \end{pmatrix} = \begin{pmatrix} a_1 & b_1 \\ d_1 & e_1 \\ g_1 & h_1 \end{pmatrix}$$

Incidence constraints In the same manner, incidence constraints may be deduced from the fact that the subdivision of the endpoints must be in harmony with endpoints of subdivided edges. Thus, for the left endpoint let us follow the paths $e \xrightarrow{b_0} e \xrightarrow{T_v} v = e \xrightarrow{T_0} e \xrightarrow{b_0} v$, what results into the constraint $b_0 T_v = T_0 b_0$. The same holds for the right endpoint: $b_1 T_v = T_1 b_1$, the constraints are shown in red in figure 5. If the constraints are not fulfilled we will get a disconnected curve after two subdivisions. Let us solve the constraints on the matrices. Having denoted $T_v = \begin{pmatrix} a_v & b_v \\ d_v & e_v \end{pmatrix}$ we get:

$$\begin{pmatrix} 1 & 0 \\ 0 & 1 \\ 0 & 0 \end{pmatrix} \begin{pmatrix} a_v & b_v \\ d_v & e_v \end{pmatrix} = \begin{pmatrix} a_0 & b_0 & c_0 \\ d_0 & e_0 & f_0 \\ g_0 & h_0 & i_0 \end{pmatrix} \begin{pmatrix} 1 & 0 \\ 0 & 1 \\ 0 & 0 \end{pmatrix}$$

$$\begin{pmatrix} a_v & b_v \\ d_v & e_v \\ 0 & 0 \end{pmatrix} = \begin{pmatrix} a_0 & b_0 \\ d_0 & e_0 \\ g_0 & h_0 \end{pmatrix}$$

and

$$\begin{pmatrix} 0 & 0 \\ 1 & 0 \\ 0 & 1 \end{pmatrix} \begin{pmatrix} a_v & b_v \\ d_v & e_v \end{pmatrix} = \begin{pmatrix} a_1 & b_1 & c_1 \\ d_1 & e_1 & f_1 \\ g_1 & h_1 & i_1 \end{pmatrix} \begin{pmatrix} 0 & 0 \\ 1 & 0 \\ 0 & 1 \end{pmatrix}$$

$$\begin{pmatrix} 0 & 0 \\ a_v & b_v \\ d_v & e_v \end{pmatrix} = \begin{pmatrix} b_1 & c_1 \\ e_1 & f_1 \\ h_1 & i_1 \end{pmatrix}$$

Then it easy to see that:

$$T_0 = \begin{pmatrix} a_s & b_s & 0 \\ d_s & e_s & a_s \\ 0 & 0 & e_s \end{pmatrix} \quad T_1 = \begin{pmatrix} b_s & 0 & 0 \\ e_s & a_s & b_s \\ 0 & d_s & e_s \end{pmatrix}$$

Let us add the fact that the matrices are stochastic (all columns sum up to 1) and we see that for a local corner cutting curve whose points depend on at most three control points (and on two at least) there are only two degrees of freedom:

$$T_0 = \begin{bmatrix} 1-a & b & 0 \\ a & 1-b & 1-a \\ 0 & 0 & a \end{bmatrix} \quad T_1 = \begin{bmatrix} b & 0 & 0 \\ 1-b & 1-a & b \\ 0 & a & 1-b \end{bmatrix}$$

Convergence The convergence theorem [1] states that in order to get the convergence of an IFS with linear transformations the operators must have eigenvalues strictly less than 1 (in absolute value) with one exception: all stochastic operators have eigenvalue 1 that correspond to fixed points of the operators. T_0 has eigenvalues: $(1, a, 1 - a - b)$, while T_1 has $(1, b, 1 - a - b)$. Thus in our case the convergence holds if and only if:

$$\begin{aligned} -1 &< a < 1 \\ -1 &< b < 1 \\ -1 &< 1 - a - b < 1 \end{aligned}$$

Local corner cutting curves were studied earlier by Gregory, Qu, De Boor et al [8, 5, 14]. The notations we use here correspond exactly to their works, however there is a difference in the domain of definition. In fact, when the cited authors construct corner cutting curves, they suppose that all vertices of a polygon at iteration n belong to the polygon from the iteration $n - 1$. Therefore, the studied domain is shown in gray in figure 6, it corresponds to the domain with positive eigenvalues a, b and $1 - a - b$. Our construction does not use this assumption, so the domain we study here is all the region of convergence (shown in red).

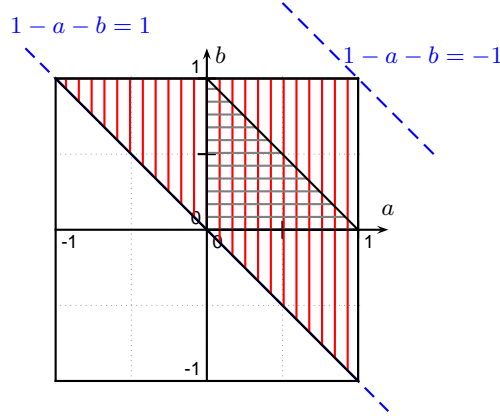


Fig. 6. In red: the domain of convergence, in gray: Gregory-Qu domain of definition.

Parameterization and self-similarity Under latter constraints the attractor of the IFS $\{T_0, T_1\}$ is a curve in three-dimensional barycentric space. It is easy to parameterize the curve with so-called natural parameterization $t \in [0, 1]$, where $t = 0$ corresponds to the “left” endpoint of the curve, $t = 1$ is the “right” endpoint and $t = \frac{1}{2}$ corresponds to the junction point in the first level of subdivision.

Then if we denote the parameterized curve (in the barycentric space) as $F(t)$, it is easy to get the parameterized curve in the modelling space $C(t) = PF(t)$, where $P = (P_0 \ P_1 \ P_2)$ is the vector of control points. Let us rewrite the self-similarity property of the curve: $F([0, \frac{1}{2}]) = T_0F([0, 1])$ and $F([\frac{1}{2}, 1]) = T_1F([0, 1])$. The parameterization is induced by the subdivision of the parameter space $[0, 1]$ for each iteration.

4 Differentiability

Half-tangent vectors at endpoints are defined for large class of fractal curves [3]. Attractors are self-similar, so if a half-tangent \vec{v} exists for $t = 0$ then it is easy to find a half-tangent vector for $t = \frac{1}{2}$: vector $T_1\vec{v}$ is tangent to the curve $F([\frac{1}{2}, 1]) = T_1F([0, 1])$. Therefore, having defined half-tangent vectors for endpoints of a fractal curve we automatically define it for a set dense in the parameter domain. In the same way if a fractal curve is not differentiable for an endpoint the singularity is copied by the self-similarity property.

4.1 Eigenvectors and eigenvalues

T_0 has real eigenvalues $\lambda_0^0 = 1$, $\lambda_1^0 = 1 - a - b$, $\lambda_2^0 = a$ and T_1 has $\lambda_0^1 = 1$, $\lambda_1^1 = 1 - a - b$, $\lambda_2^1 = b$. Corresponding eigenvectors are:

$$\vec{v}_0^0 = \begin{pmatrix} \frac{b}{a+b} \\ \frac{a}{a+b} \\ 0 \end{pmatrix}, \vec{v}_1^0 = \begin{pmatrix} 1 \\ -1 \\ 0 \end{pmatrix}, \vec{v}_2^0 = \begin{pmatrix} -b \\ 1 - 2a \\ 2a + b - 1 \end{pmatrix}$$

and

$$\vec{v}_0^1 = \begin{pmatrix} 0 \\ \frac{b}{a+b} \\ \frac{a}{a+b} \end{pmatrix}, \vec{v}_1^1 = \begin{pmatrix} 0 \\ 1 \\ -1 \end{pmatrix}, \vec{v}_2^1 = \begin{pmatrix} a+2b-1 \\ 1-2b \\ -a \end{pmatrix}$$

Eigenvectors v_0^0 and v_0^1 corresponding to the eigenvalue 1 give fixed points of T_0 and T_1 . Note that the fixed points are endpoints of the curve: $v_0^0 = F(0)$ and $v_0^1 = F(1)$. It is easy to see that eigenvectors corresponding to the sub-dominant eigenvalues give half-tangents to the endpoints. Note that sub-dominant eigenvalues of T_0 and T_1 are non negative.

There are four cases:

1. $1-a-b$ is the sub-dominant eigenvalue of T_0 : $|1-a-b| \geq |a| \Rightarrow 1-2a-b \geq 0$.
In such a case the half-tangent to $F(0)$ is collinear with $(1-1\ 0)^\top$ and the half-tangent to $C(0)$ is collinear with $\vec{P_0 - P_1}$.
2. a is the sub-dominant eigenvalue of T_0 : $|a| > |1-a-b| \Rightarrow 1-2a-b < 0$.
In this case the half-tangent to $C(0)$ is $-bP_0 + (1-2a)P_1 + (2a+b-1)P_2$.
This vector can have different orientations depending on the values of a and b .
3. $1-a-b$ is the sub-dominant eigenvalue of T_1 : $|1-a-b| \geq |b| \Rightarrow 1-a-2b \geq 0$.
The half-tangent to $C(1)$ is collinear with $\vec{P_1 - P_2}$.
4. b is the sub-dominant eigenvalue of T_1 : $|b| > |1-a-b| \Rightarrow 1-a-2b < 0$.
The half-tangent to $C(1)$ has direction $(a+2b-1)P_0 + (1-2b)P_1 - aP_2$.
Again, the direction depends on a and b .

The most interesting case is when $1-a-b$ is the sub-dominant eigenvalue for both T_0 and T_1 . In such a case half-tangents are given by two control points and therefore their directions do not depend on a and b .

4.2 Necessary conditions for differentiability

Incidence and adjacency constraints of the BC-IFS guarantee C^0 continuity for the limit curve. To have C^1 continuity half-tangents must be collinear at the junction point. Figure 7 shows an illustration.

Let us suppose that the curve is differentiable, the half-tangents for the point $t = \frac{1}{2}$ may be obtained by the self-similarity property from the half-tangents to endpoints. If \vec{t}_- and \vec{t}_+ are the directions of the half-tangents to endpoints, then $T_1\vec{t}_+$ must be equal to $T_0\vec{t}_-$:

$$\begin{aligned} C([0, 1]) &= (Q_0\ Q_1\ Q_2)F([0, 1]) \cup (Q_1\ Q_2\ Q_3)F([0, 1]) \\ &= PT_0F([0, 1]) \cup PT_1F([0, 1]) \end{aligned}$$

As we have mentioned previously, vectors \vec{t}_+ and \vec{t}_- depend on values of a and b . To have G^1 continuity, it is obvious that $T_1\vec{t}_+$ and $T_0\vec{t}_-$ must be (at

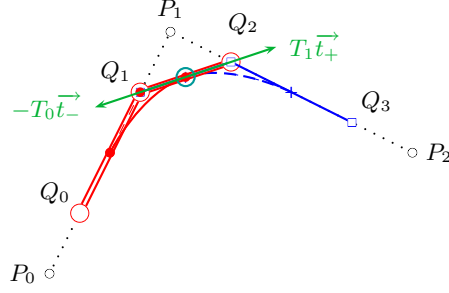


Fig. 7. Half-tangent vectors at the joining point.

least) collinear for any configuration of control points $(Q_0 Q_1 Q_2 Q_3)$. The only possibility to fulfil the collinearity is when²:

- vector \vec{t}_- belongs to the subspace corresponding to control points P_1 and P_2 , i.e. has zero first component. This is the case iff $1 - 2a - b > 0$.
- vector \vec{t}_+ belongs to the subspace corresponding to control points P_0 and P_1 , i.e. has zero third component. This is the case iff $1 - a - 2b > 0$.

Therefore if $T_1\vec{t}_-$ and $T_0\vec{t}_+$ are collinear, then $1 - a - b$ is sub-dominant eigenvalue for both T_0 and T_1 . The corresponding domain is shown by hatching in red and blue in figure 8. However it is a *necessary* condition: it includes regions of differentiability (zone 1) as well as regions of cusp points (zones 2 and 2'). Therefore, collinearity is a rough tool and to distinguish the zones we have to find direction of tangent vectors.

4.3 Cartography of differential behaviours

To find direction of half-tangents and to identify differential behaviour of the other areas in the convergence domain, we use the following property established in [2].

Property 1. Let us find decomposition of $\overrightarrow{F(0)F(1)}$ in the eigenbases of T_0 and T_1 , respectively:

$$\begin{aligned}\overrightarrow{F(0)F(1)} &= \alpha_1 \vec{v}_1^0 + \alpha_2 \vec{v}_2^0 = \frac{(-b)(a+b-1)}{(2a+b-1)(a+b)} \vec{v}_1^0 + \frac{a}{(2a+b-1)(a+b)} \vec{v}_2^0 \\ \overrightarrow{F(0)F(1)} &= \beta_1 \vec{v}_1^1 + \beta_2 \vec{v}_2^1 = \frac{(-a)(a+b-1)}{(a+2b-1)(a+b)} \vec{v}_1^1 + \frac{-b}{(a+2b-1)(a+b)} \vec{v}_2^1\end{aligned}$$

Let $R, L \in \{1, 2\}$ such that v_L^0 and v_R^1 are the sub-dominant eigenvectors of T^0 and T^1 , respectively. Then if $F(t)$ has left and right half-tangents at

² Except degenerated cases: if $a = 0$ or $b = 0$ or $a + b = 1$ then the curve is degenerated (piecewise linear) and therefore differentiable (except at vertices).

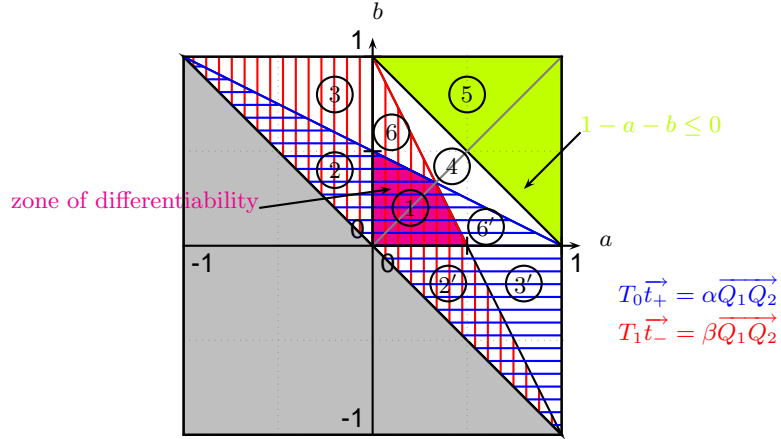


Fig. 8. Cartography of regions according to differential properties.

respectively $F(1)$ and $F(0)$, their directions \vec{t}_- and \vec{t}_+ are given by:

$$\begin{aligned} \vec{t}_- &= \alpha_L \vec{v}_L^0 \\ \vec{t}_+ &= \beta_R \vec{v}_R^1 \end{aligned}$$

Let us consider the subdivision of the curve :

$$C([0, 1]) = (Q_0 Q_1 Q_2) F([0, 1]) \cup (Q_1 Q_2 Q_3) F([0, 1])$$

Now we focus on the point of junction of the two sub-curves $C_0(t) = (Q_0 Q_1 Q_2) F(t)$ and $C_1(t) = (Q_1 Q_2 Q_3) F(t)$. The directions of the half-tangents at the point are given by $(Q_1 Q_2 Q_3) \vec{t}_-$ for C_0 and $(Q_0 Q_1 Q_2) \vec{t}_+$ for C_1 .

Depending on sub-dominant eigenvalues of T_0 and T_1 we can have three main different cases:

1. $1 - a - b > a$ and $1 - a - b > b$: this case covers three regions in figure 8, namely regions 1, 2 and 2'. Here we have $R = L = 1$ and

$$\begin{aligned} (Q_0 Q_1 Q_2) \vec{t}_r &= \beta_1 (Q_0 Q_1 Q_2) \vec{v}_1^1 = \beta_1 \overline{Q_1 Q_2} \\ (Q_1 Q_2 Q_3) \vec{t}_l &= \alpha_1 (Q_1 Q_2 Q_3) \vec{v}_1^0 = \alpha_1 \overline{Q_1 Q_2} \end{aligned}$$

with $\alpha_1 = \frac{(-b)(a+b-1)}{(2a+b-1)(a+b)}$ and $\beta_1 = \frac{(-a)(a+b-1)}{(a+2b-1)(a+b)}$. As was explained in the previous section, the two half-tangent vectors at the joining point are collinear in this case. However, the vectors have the same direction if and only if α_1 and β_1 are of the same sign, and it is the case for the region 1 of figure 8. For regions 2 and 2' half-tangent vectors have opposite directions, resulting into cusp points.

2. $1 - a - b > a$ or (exclusive) $1 - a - b > b$: $(Q_1 Q_2 Q_3) \vec{t}_+$ and $(Q_0 Q_1 Q_2) \vec{t}_-$ are not collinear in general case. If one of the sub-dominant eigenvalues of T_0 or T_1 is $1 - a - b$ then the corresponding half-tangent vector is collinear with $\overrightarrow{Q_1 Q_2}$ (regions 3 and 3') but the other half-tangent is not.
3. $1 - a - b < a$ and $1 - a - b < b$: this case corresponds to regions 4 and 5 of figure 8. No half-tangent vector is collinear to $\overrightarrow{Q_1 Q_2}$ since the eigenvectors have three non-zero components and therefore the half-tangent vectors depend on three control points respectively $(Q_1 Q_2 Q_3)$ and $(Q_0 Q_1 Q_2)$. Regions 4 and 5 differ in the sign of the smallest (in absolute value) eigenvalue $1 - a - b$. For the region 5 the eigenvalue is negative, and it forces the curve to oscillate around the direction of the half-tangent, thus giving a “fractal” aspect to the curve.

5 Sufficient conditions

Figure 9 shows the motivation for this section. If we use the natural parameterization, then even for differentiable curves, blending functions $F(t)$ are not differentiable in the sense of Lipschitz. However, under a suitable parameterization the blending functions are differentiable. The image is obtained for values $a = 1/20$ and $b = 1/8$.

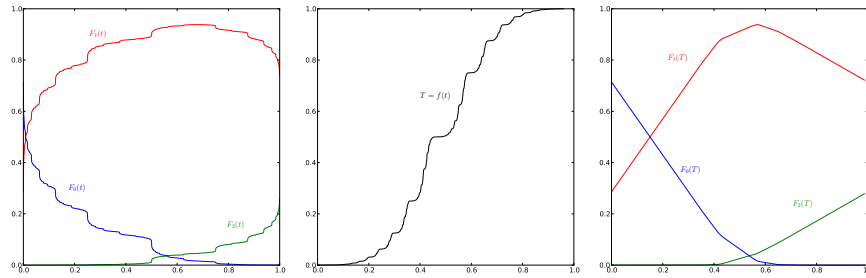


Fig. 9. Left image: The three components of blending function $F(t)$ in the natural parameterization. In the middle: non-singular parameterization as a function of natural parametrization. Right image: The three components blending function in the non-singular parameterization.

This is very similar to the situation with Stam’s method [18] of exact evaluation of subdivision surfaces. Having constructed the natural parameterization it is easy to find points of a curve (surface), however the behaviour of derivatives is erratic and therefore many methods like [10] may fail to work with this parameterization. There are several works that construct non-singular parameterizations, for example, we can cite [4] for Catmull-Clark subdivision surfaces.

In this section we will show how to reparameterize any curve from Gregory region to guarantee C^1 blending functions. So instead of subdividing the param-

eter domain in equal halves as the natural parameterization does, we follow the same subdivision rules as for the control polygon. Figure 10 illustrates the idea. We start with a control polygon (P_0, P_1, P_2) ; in order to parameterize it we chose three real values (t_0, t_1, t_2) such that $t_0 < t_1 < t_2$. Then we say that the segments (P_0, P_1) and (P_1, P_2) have linear parameter domains (t_0, t_1) and (t_1, t_2) , respectively.

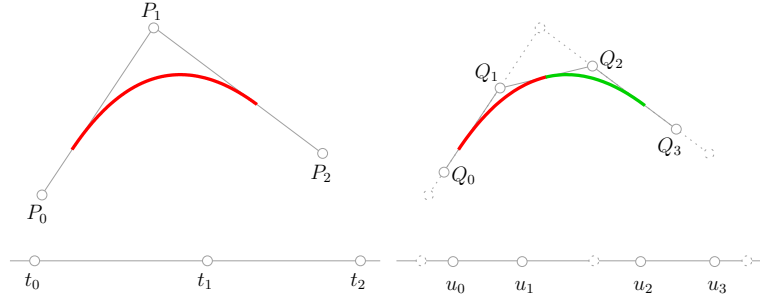


Fig. 10. Left image: original control polygon (P_0, P_1, P_2) and its parameter values (t_0, t_1, t_2) . Right image: parameter domain is subdivided along with the control polygon.

Then subdivided polygon (Q_0, Q_1, Q_2, Q_3) is parameterized with three segments (u_0, u_1) , (u_1, u_2) and (u_2, u_3) , where u_i are obtained by the same rules of subdivision as Q_i :

$$\begin{aligned} (Q_0 \ Q_1 \ Q_2) &= (P_0 \ P_1 \ P_2) T_0 & (u_0 \ u_1 \ u_2) &= (t_0 \ t_1 \ t_2) T_0 \\ (Q_1 \ Q_2 \ Q_3) &= (P_0 \ P_1 \ P_2) T_1 & (u_1 \ u_2 \ u_3) &= (t_0 \ t_1 \ t_2) T_1 \end{aligned}$$

The limit of the process gives us a well-parameterized curve. To verify the C^1 continuity of the limit curve one may proceed as follows:

- construct a sequence of functions $\{f_i\}_{i=0}^\infty$ converging pointwise to the limit function $F(t)$. Here we start with a vector of blending functions f_0 for the control polygon (P_0, P_1, P_2) . Then f_1 is the vector of blending functions for the polygon (Q_0, Q_1, Q_2, Q_3) etc.
- construct a sequence of derivatives $\{f'_i\}_{i=0}^\infty$ and show that it converges uniformly to a continuous function
- prove that the limit $\lim_{i \rightarrow \infty} f'_i$ is indeed the derivative of the curve $F(t)$

In such a way we get *sufficient* conditions for differentiability, not only necessary ones. We do not want to overload the presentation with technical questions of uniform convergence, all the proofs are detailed in a technical report [17]. The report proves that a curves is C^1 continuous if and only if a and b are located in the Gregory region (magenta zone in figure 8).

Moreover, we have proved that for *any* a and b in the convergence domain limit curves are differentiable *almost everywhere*, i.e. everywhere except on a set of measure zero [17]. As a matter of fact, this set consists of the junction point under all possible finite sequences of applications T_0 and T_1 . In other words, in the natural parameterization it is the point $t = \frac{1}{2}$, $t = \frac{1}{4}$, $t = \frac{3}{4}$ etc (all points of dyadic parameters). This set is denumerable.

6 Roughness of a curve

There are few ways to describe roughness of a curve like Hölder exponent and fractal dimension. All the descriptors are good per se, but a curve may be fully described only by combining descriptors. Here we introduce a new descriptor, namely angles between half-tangent vectors $T_0\vec{t}_-$ and $T_1\vec{t}_+$.

So we know that any curve from the Gregory-Qu domain is differentiable, but if we are not very far from the domain; curves are not very rough either. These “almost smooth” curves may be a good fit for computer graphics, where all geometry is discretized anyway. Or if one searches look for a really rough curve, where to look for it in the convergence domain? Angles between half-tangent vectors are very easy to calculate, and therefore the search is very efficient:

$$\alpha(a, b) = \arccos \frac{\langle T_0\vec{t}_-, T_1\vec{t}_+ \rangle}{\|T_0\vec{t}_-\| \|T_1\vec{t}_+\|}$$

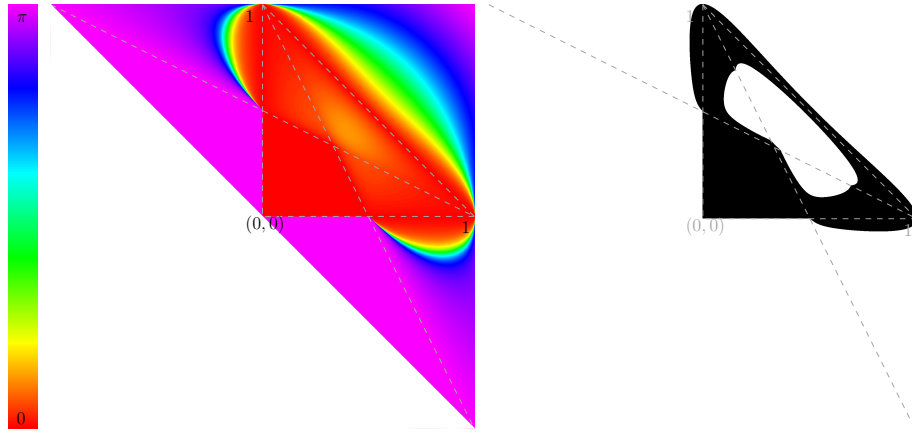


Fig. 11. Left image: angle between two half-tangent vectors from 0 (red) to π (violet); right image: thresholded version of the left one, the domain represents “almost smooth” curves (the angle is less than 5 degrees).

Left image of figure 11 shows a graph of roughness vs values of a and b . The domain of Gregory-Qu is marked in red as half-tangent are collinear (note that

degenerate cases $a = b$, $b = 0$ and $1 = a + b$ are also in red). All cusp points are marked in violet. Right image shows a thresholded version of the left one. Here we have selected threshold of 5° , so any curve generated with a and b from the black region is guaranteed to be “almost smooth”.

7 Conclusion

Up to this moment we have shown how a curve may be constructed. Constructing a surface may be done in exactly the same manner. For example, Doo-Sabin subdivision scheme may be described as a face-edge-vertex B-rep, where a patch (topological “face”) is bounded by four “edges”. Then each patch is subdivided into four smaller sub-patches and all them may be stitched together by implying adjacency of corresponding borders. Then it is immediate that for a (regular) Doo-Sabin patch there are three degrees of freedom. Either we set it to classic values $(0.5625, 0.1875, 0.1875)$ to get the Doo-Sabin subdivision surface, either we look for other shapes (either smooth and differentiable or not). Figure 12 shows six different surfaces obtained by subdividing a cube with different triples of weights.

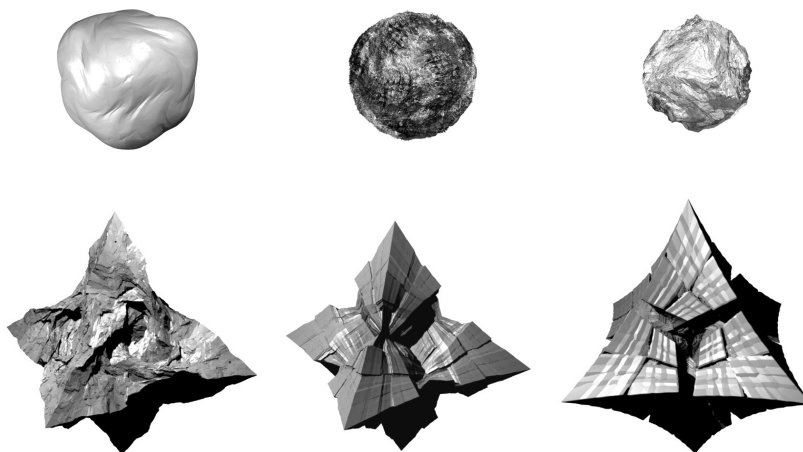


Fig. 12. Examples of different “*geometric textures*” obtained obtained by subdividing a cube with different subdivision weights.

In this paper we have presented how to model curves and surfaces by means of iterative process, namely linear BC-IFS (Boundary Controlled Iteratif Function System). This approach guarantees the required topology of the final shape by introducing incidence and adjacency constraints on a B-Rep model. For an linear BC-IFS it implies constraints on underlying matrices representing subdivision operators.

In this paper we have explicitly constructed local corner cutting curves and studied the differential behaviour by analyzing eigenvalues and eigenvectors of the subdivision operators. While we find some necessary conditions as do Gregory and De Boor, we study a larger family of curves, since by using BC-IFS approach we are able to enrich the convergence domain, thus introducing new shapes. To characterize different families of shapes in the convergence domain we study eigenstructures of subdivision operators and propose a precise cartography of all the regions.

We have also proved that necessary conditions are also sufficient ones. Moreover, we have proved that stationary local corner cutting curves are differentiable *almost everywhere*.

Finally, we have proposed a new roughness descriptor of fractal shapes. With this descriptor it is immediate to see where in the convergence domain we have to look for rough or smooth curves. Indeed, even if a curve is not differentiable it may look very smooth.

References

1. Michael Barnsley. *Fractals everywhere*. Academic Press Professional, Inc., San Diego, CA, USA, 1988.
2. Hicham Bensoudane. *Étude différentielle des formes fractales*. PhD thesis, Université de Bourgogne, 2009.
3. Hicham Bensoudane, Christian Gentil, and Marc Neveu. Fractional half-tangent of a curve described by iterated function system. *Journal Of Applied Functional Analysis*, 4(2):311–326, April 2009.
4. Ioana Boier-Martin and Denis Zorin. Differentiable parameterization of Catmull-Clark subdivision surfaces. In *SGP '04: Proceedings of the 2004 Eurographics/ACM SIGGRAPH symposium on Geometry processing*, pages 155–164, New York, NY, USA, 2004. ACM.
5. Carl De Boor. Local corner cutting and the smoothness of the limiting curve. *Computer Aided Geometric Design*, 7(5):389 – 397, 1990.
6. Wayne O. Cochran, Robert R. Lewis, and John C. Hart. The normal of a fractal surface. *The Visual Computer*, 17(4):209–218, June 2001.
7. Christian Gentil. *Les fractales en synthèse d'image : le modèle IFS*. PhD thesis, Université LYON 1, 1992.
8. John A. Gregory and Ruibin Qu. Nonuniform corner cutting. *Computer Aided Geometric Design*, 13(8):763 – 772, 1996.
9. John Hutchinson. Fractals and self-similarity. *Indiana University Journal of Mathematics*, 30(5):713–747, 1981.
10. Andrei Khodakovsky and Peter Schröder. Fine level feature editing for subdivision surfaces. In *SMA '99: Proceedings of the fifth ACM symposium on Solid modeling and applications*, pages 203–211, New York, NY, USA, 1999. ACM.
11. K.M. Kolwankar and A. D. Gangal. Hölder exponents of irregular signals and local fractional derivatives. *Pramana*, 48(1):49–68, January 1997.
12. K.M. Kolwankar and A.D. Gangal. Local fractional derivatives and fractal functions of several variables. *in: Proc. of Fractals in Engineering*, 1997.
13. R. Daniel Mauldin and S. C. Williams. Hausdorff dimension in graph directed constructions. *Transactions of the American Mathematical Society*, 309(2):811–829, 1988.

14. Marco Paluszny, Hartmut Prautzsch, and Martin Schäfer. A geometric look at corner cutting. *Computer Aided Geometric Design*, 14(5):421 – 447, 1997.
15. Przemyslaw Prusinkiewicz and Mark S. Hammel. Language-restricted iterated function systems, koch constructions and l-systems. In *New Directions for Fractal Modeling in Computer Graphics, ACM SIGGRAPH Course Notes*. ACM Press, 1994.
16. Robert Sealey. *V -variable fractals and interpolation*. PhD thesis, Australian National University, 2008.
17. Dmitry Sokolov and Christian Gentil. Sufficient conditions for differentiability of local corner cutting curves. Research report, LE2I, Université de Bourgogne, 2010.
18. Jos Stam. Exact evaluation of Catmull-Clark subdivision surfaces at arbitrary parameter values. In *Proceedings of SIGGRAPH*, pages 395–404, 1998.
19. E. Tosan, I. Bailly-Sallins, G. Gouaty, I. Stotz, P. Buser, and Y. Weinand. Une modélisation géométrique itérative basée sur les automates. In *GTMG 2006, Journées du Groupe de Travail en Modélisation Géométrique, Cachan*, pages 155–169, 22-23 Mars 2006.
20. Chems Eddine Zair and Eric Tosan. Fractal modeling using free form techniques. *Computer Graphics Forum*, 15(3):269–278, 1996.